Applied Physics B (2020) 126:134
https://doi.org/10.1007/s00340-020-07485-6

Applied Physics B
Lasers and Optics

A fully stabilized low-phase-noise Kerr-lens mode-locked Yb:CYA laser frequency comb with an average power of 1.5 W

Ziyue Zhang[1,2] · Hainian Han[1] · Wenlong Tian[3] · Xiaodong Shao[1,2] · Huibo Wang[3] · Xiaodong Xu[5] · Zhiyi Wei[1,2,3,4]

Received: 1 March 2020 / Accepted: 7 July 2020 / Published online: 18 July 2020

Abstract

We report a fully stabilized self-referenced all-solid-state-laser frequency comb based on a home-built Kerr-lens mode-locked $Yb:CaYAlO_4$ oscillator, which delivers ultrafast pulses with a pulse duration of 54 fs and an average power of 1.5 W. Free running carrier-envelope phase offset frequency (f_{ceo}) is observed with a signal to noise ratio of 40 dB at 100 kHz resolution bandwidth, which is phase-locked to a microwave frequency synthesizer with a residual phase jitter of 370 mrad [1 Hz–1 MHz] and with a standard frequency deviation of 0.8 mHz at 1-s gate time within 3-h, corresponding to the relative frequency instability of 2.9×10^{-18} at 1-s average time. It is the lowest phase noise and the highest frequency stability of f_{ceo} obtained in a watt-level all-solid-state bulk laser frequency comb to the best of our knowledge. A 13th repetition rate is simultaneously phase-locked to the same microwave standard with a frequency instability level of 10^{-12} at 1 s average time. Such fully stabilized power scaling Yb: $CaYAlO_4$ laser frequency combs have great potential for applications in broadband dual comb spectroscopy as well as high loss cases such as long-distance time and frequency transfer.

1 Introduction

Power scaling watt-level near infrared (NIR) optical frequency combs (OFCs) with full stabilization of repetition frequency and carrier-envelope phase offset frequency (f_{ceo}) have made great progresses in precision frequency metrology and high resolution frequency comb spectroscopy [1–3]. High energy NIR frequency combs can also be competitive candidates for driving nonlinear frequency conversion processes to extend the broadband spectroscopy to spectral regions where no suitable laser radiation exits such as mid-infrared and ultraviolet frequency ranges, which benefits researches on molecular and atomic transitions and structures, and enables lots of practical applications including trace gas monitoring and hyperspectral imaging [4–8]. Moreover, Up to 70 dB link loss in comb-based optical two way time and frequency transfer over long-distance free space also calls for ultralow-noise high power NIR OFCs [9, 10].

Several kinds of ultrafast lasers are able to generate high power OFCs, such as fiber lasers, thin disk lasers as well as all-solid-state bulk lasers. Take the fiber laser as an example, the output power could be stacked with cascaded pulse amplifier stages, but amounts of intensity noise and phase noise are also accumulated while traveling through the long-distance fibers with high nonlinearity and high order dispersion [11]. Thin disk lasers are well known as the third-generation laser technology for producing high average powers [12]. Norbert modsching et al. reported a f_{ceo} stabilized $Yb:Lu_2O_3$ thin disk laser with an average power of 4.4 W [13]. Sebastian Grobmeyer et al. have demonstrated a f_{ceo} stable 100 W-level femtosecond thin-disk oscillator with a multi-pass-cell compression stage [14]. All-solid-state bulk laser frequency combs are capable of delivering high power pulses with low cost and low intrinsic noise and high

✉ Hainian Han
hnhan@iphy.ac.cn

Zhiyi Wei
zywei@iphy.ac.cn

1 Beijing National Laboratory for Condensed Matter Physics, Institute of Physics, Chinese Academy of Sciences, Beijing 100190, China

2 School of Physical Sciences, University of Chinese Academy of Sciences, Beijing 100049, China

3 School of Physics and Optoelectronics Engineering, Xidian University, Xi'an 710071, China

4 Songshan Lake Materials Laboratory, Dongguan 523808, Guangdong, China

5 Jiangsu Key Laboratory of Advanced Laser Materials and Devices, School of Physics and Electronic Engineering, Jiangsu Normal University, Xuzhou 221116, China

efficiency. Compared to the fiber lasers and thin disk lasers, it is easily to approach high repetition rate with flexible cavity alignment and short pulse duration without any amplifier and compression stages. Therefore, impressive progresses have been enabled on various all-solid-state lasers in recent years [15–17]. However only a few Ytterbium-doped bulk lasers yielding watt-level output power have been demonstrated with both carrier-envelope phase offset (CEO) frequency and repetition rate frequency stabilized.

In 2011, Tadas Balciunas et al. reported a carrier-envelope phase stabilized Yb:KGW laser with an output power of 600 mW, serving as a seed for the subsequent amplifiers [18]. In 2013, a f_{ceo} stabilized Yb:KYW laser frequency comb was demonstrated with an average power of 300 mW, and another fiber amplification and compression stages had to be employed to obtain a narrow pulse duration of 113 fs [19]. Ytterbium-doped calcium aluminate crystal (Yb:CYA) is a promising medium with a broad emission bandwidth with 77 nm full width at half maximum (FWHM), and good thermal conductivity [20]. Several impressive works have been reported based on Yb:CYA bulk medium, such as the short pulse output with the record pulse duration of 21 fs [21] and the high power extraction with an average power of up to 6.2 W [22], which makes it an attractive candidate gain medium for developing all-solid-state laser frequency comb. We have demonstrated a Kerr lens mode locked (KLM) Yb: CYA bulk laser frequency combs with a residual carrier-envelope phase jitter of 79.3 mrad and a standard out-of-loop CEO frequency deviation of 12.95 mHz. But the output power is limited to 200 mW and the long-term frequency stability is weakly controlled in the feed forward scheme due to lack of the integration module [23]. Until 2017, a fully stabilized Semiconductor Saturable Absorber Mirror (SESAM) mode locked Yb:CALGO bulk laser was presented with an average power of 2.1 W and the pulse duration of 96 fs, where the residual phase noise of the locked f_{ceo} was 680 mrad and the overlapped Allan deviation of f_{ceo} was more than 0.3 Hz [24]. For high power femtosecond mode locked lasers, it is more challenging to obtain low-noise phase stabilization and long-term frequency stability. One reason is that amounts of intensity noises of the pump source are inevitably inserted into the laser cavity as we inject higher pump power, and are thus transferred into phase noise, leading to an increase of the linewidth of the free running f_{ceo}. Another is that it is more difficult to manage the high nonlinearity and dispersion in a high power laser cavity to obtain an ultrashort pulse duration, so the resulted increased intra-cavity quantum noise would degrade the coherence during the pulse formation as well as the supercontinuum generation process [25, 26]. Usually, SESAM mode locking technique limits the achieved ultrashort pulse width to sub-100 fs owing to the slow gain narrow effect, while Kerr-lens mode-locking scheme benefiting from ultrafast self-focusing principle could generate ultrashort pulses blow 60 fs. To a certain extent, KLM femtosecond lasers would exhibit lower intrinsic noise than the SESAM mode locked lasers [27, 28].

In this paper, we report a fully stabilized KLM Yb:CYA bulk laser frequency comb providing an average power of 1.5 W with a pulse duration of 54 fs. An octave spanning supercontinuum is obtained with high coherence in a piece of photonic crystal fiber (PCF). The residual phase jitter of the locked f_{ceo} is calculated to be 370 mrad from 1 Hz to 1 MHz. The RMS of frequency deviation of stabilized CEO frequency is 0.8 mHz within 3-h, which is the lowest phase noise and the best long-term performance of the 1-um watt-level solid state bulk laser frequency comb to the best of our knowledge and presents a significant improvement in the power extraction and frequency stability.13th harmonic of the repetition rate frequency is phase-locked at the same time with the RMS of the frequency deviation of 1.29 mHz. In addition, a complete analysis for dynamic response of the laser system is performed in terms of transfer functions.

2 High power Kerr-lens mode-locked Yb:CYA laser

2.1 Kerr-lens mode-locked Yb:CYA laser

The presented all-solid-state bulk laser frequency comb is based on a home-built KLM Yb: $CaYAlO_4$ laser, as shown in Fig. 1. A 4.3 mm-thick a-cut 3 at. % doped Yb:$CaYAlO_4$ (Yb: CYA) crystal wrapped with indium foil is mounted on a heat sink at a temperature of 14 °C, serving as the gain medium and the Kerr medium. A fiber laser radiating

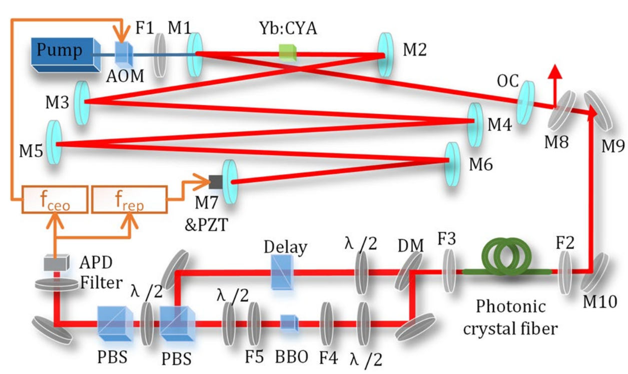

Fig. 1 Experimental setup of the fully stabilized high power KLM Yb:CYA laser frequency comb. *F1-F5* spherical lens, *M1-M2* Concave high reflective mirror, *M3-M7* high reflective mirror, *M3&M7&M9* Gires-Tournois interferometers (GTIs), *OC* output coupler with transmission of 10%, *M8* power splitter, *M10* silver mirror, *AOM* acousto-optic modulator; *DM* dichroic mirror, *PBS* polarization beam splitter, *λ/2* half-wavelength plate, *Delay* delay stages, *APD* avalanche photo diode

980 nm with a maximum output power of 9.2 W is used as the pump source. With an appropriate imaging system, the pump power is focused into the anti-reflective coated gain medium with a spot diameter of 60 μm. A standard X-fold cavity is aligned. The concave mirrors M1 and M2 with a radius of curvature of 100 mm are dichroic mirrors with high-reflection coatings in the range of 1000–1100 nm and high-transmission coatings in the range of 960–980 nm. Three Gires–Tournois Interferometer (GTI) mirrors provide 1175 fs^2 negative group velocity dispersion per bounce for dispersion compensation.

Once the Kerr-lens mode-locking is initiated through tapping the end mirror M7 mounted on a high-precision translation stage, an average power of 1.5 Watts is extracted from the output coupler with a transmission of 10%, exhibiting an optical to optical efficiency of 16.67%. The pulse duration of the direct output pulses is measured to be 67 fs and is compressed to 54 fs by use of a piece of GTI mirror with a negative group velocity dispersion of 800 fs^2. The second-harmonic autocorrelation measurement and sech^2 fitting pulse duration are shown in Fig. 2a. The corresponding

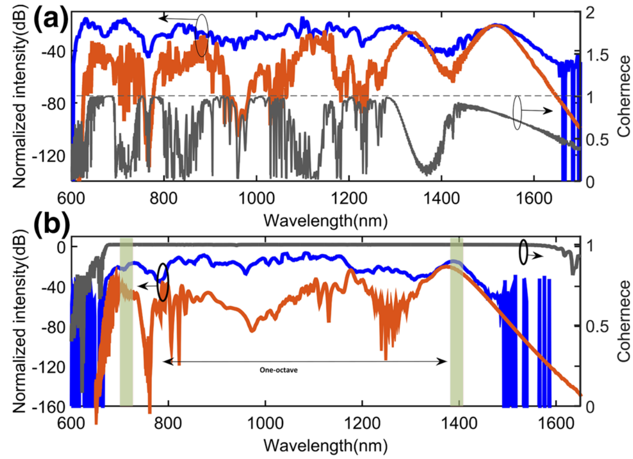

Fig. 3 The simulated (orange) and measured (blue) supercontinuum generated from NKT SC-3.7-975 PCF with 330 mW (**a**) and 80 mW (**b**) injection, the first-order of coherence is shown in gray line relative to the right axis

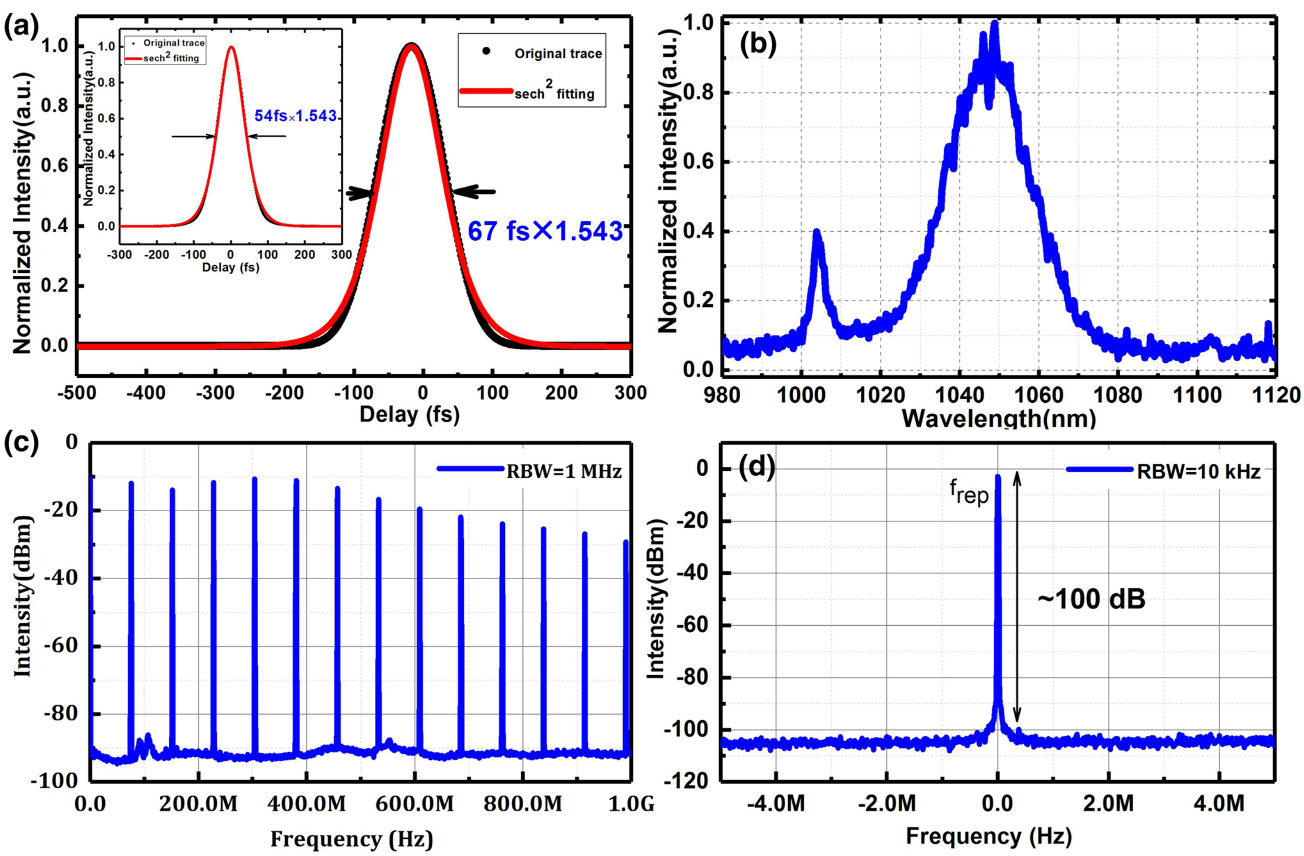

Fig. 2 **a** The measured autocorrelation and sech^2 fitting of the direct output and after-compression(inset); **b** Kerr-lens mode-locked output spectrum; **c** the measured radio frequency (RF) spectrum of Kerr-lens mode-locked Yb:CYA laser pulse within 1 GHz span under 1 MHz RBW; **d** RF spectrum of pulse train under 10 kHz RBW

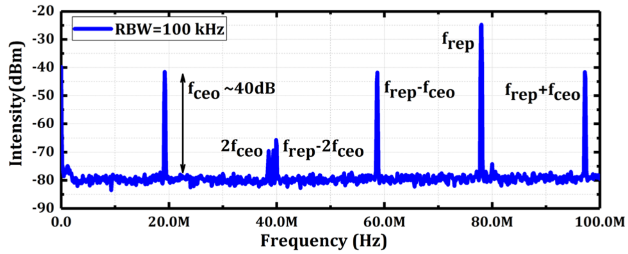

Fig. 4 RF spectrum of f_{ceo} beat signal with 40 dB SNR under 100 kHz RBW detected at the end of self-referenced f-2f interferometer. f_{rep} repetition rate. f_{ceo} carrier-envelope phase offset frequency

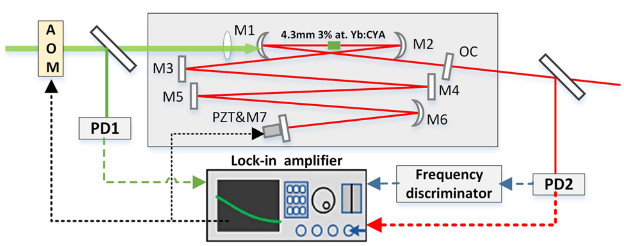

Fig. 5 Schematic of transfer function (TF) measurement. The gray frame: Laser cavity. M1-M7: laser cavity mirror. OC: output coupler. AOM: acousto-optic modulator. PZT: Piezo-electric Transducer. PD: photodiode. Black dashed line: input scanning voltage. Green dashed line: TF of AOM. Red dashed line: TF of the laser cavity. Blue dashed line: TF of the PZT

optical spectrum centered at 1048 nm is 26 nm Full Width at Half Maximum (FWHM), as shown in Fig. 2b. Figure 2c shows the radio frequency (RF) spectrum of the pulse trains recorded by a frequency spectrum analyzer (R&S, FSW 26). The fundamental repetition rate is 78 MHz with a signal to noise ratio (SNR) of more than 100 dB at the resolution bandwidth (RBW) of 10 kHz. Frequency sequences over 1 GHz span are also observed under 1 MHz RBW, indicating a stable Kerr-lens mode-locking operation. The resulting pulse energy is 19 nJ and the peak power reaches 352 kW.

2.2 Supercontinuum generation and CEO frequency detection

In order to obtain an octave spanning spectrum for the f_{ceo} detection, we launch a fraction of the output power into a 1-m long nonlinear photonic crystal fiber (PCF, NKT Photonics, SC-3.7-975) with a mode field diameter of 3.2 μm and a nonlinear coefficient of 18 $(\mathrm{W\ km})^{-1}$ at 1060 nm. Firstly, a half of the output power split with a 50% power beam splitter is injected into the PCF, and a 330 mW supercontinuum (SC) spanning from 600 to 1600 nm is obtained with a coupling efficiency of 45%, as shown in Fig. 3a. The measured SC spectrum shows good agreement with the simulation results of SC generation with the same pulse energy injection, which is performed through solving the generalized nonlinear Schrodinger equation by use of a commercial software-Fiber desk. However, the signal to noise ratio (SNR) of the detected f_{ceo} in this condition is no more than 20 dB at 100 kHz RBW, and the intensity of the CEO beat signal is quite unstable. Explanations can be found in the simulation results of the first-order spectra coherence, which displays a relative low coherence at several octave spanning spectra peaks with 330 mW injection. According to the incoherent regime of input pulse soliton order reported in Ref [25], soliton order should be degraded in order to enhance the spectral coherence. Therefore, we reduce the input average power to 150 mW by use of a piece of 10% power beam splitter. An octave spanning spectrum covering from 700 to 1400 nm with an average power of 80 mW is obtained, which is matched with the simulated SC generation, as shown in Fig. 3b. The calculated spectral coherence is also close to 1, representing a high degree coherence for the f_{ceo} detection.

The SC is then launched into a standard self-referenced f-2f interferometer to detect the f_{ceo} beat signal. A dichroic mirror is used to separate the long wavelength centered at 1400 nm from the short wavelength component centered at 700 nm. Frequency doubling process is achieved by a piece of Barium metaborate (BBO) crystal while temporal delay between the fundamental and second-harmonic short wavelength is compensated by a pair of rectangular prisms. Both the fundamental and frequency doubled short wavelength beams centered at 700 nm recombine through a pair of PBSs and several pieces of half-wavelength plates. CEO beat signal is detected by an avalanche photodiode (APD) and a frequency spectrum analyzer (R&S, FSW 26) after an optical bandpass filter at the end of the f-2f interferometer. We obtained a strong CEO beat signal with a signal to noise ratio (SNR) of 40 dB under 100 kHz resolution bandwidth (RBW), as shown in Fig. 4. The second harmonic f_{ceo} is also observed in the RF spectrum.

2.3 Cavity transfer function

In our experiments, we use a commercial 980 nm fiber laser as the pump source, which is based on an ytterbium-doped fiber master oscillator power amplifier (MOPA) configuration. An acousto-optic modulator (AOM) is injected into the pump beam to serve as a carrier-envelope phase locking actuator since there is no fast modulation module in the pump power supply and the ytterbium-doped MOPA would filter the high frequency modulation as well. In order to characterize the dynamic response from the AOM to the f_{ceo} variation in the Yb: CYA KLM laser, we investigate the transfer functions of the laser systems with a HF2LI lock-in amplifier

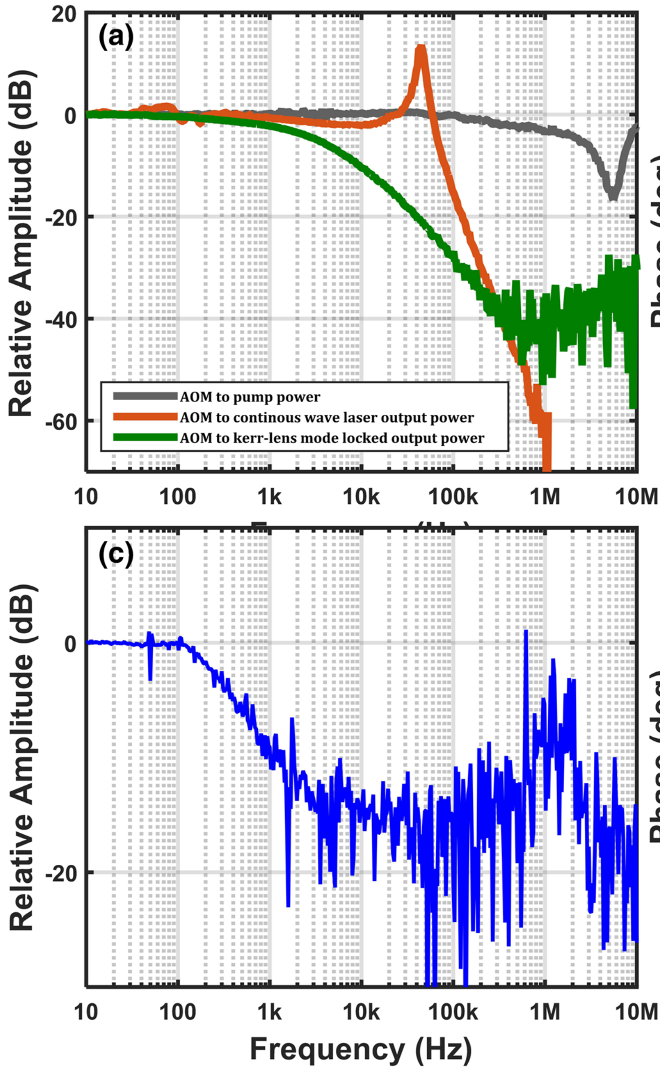

Fig. 6 **a** Relative amplitude and **b** phase response of the Yb:CYA laser output for the modulation of the pump power are shown in AOM (gray) and in continuous-wave (orange) and mode-locked laser (green) operation. Transfer functions of PZT in terms of repetition rate frequency are shown in relative amplitude (**c**) and phase (**d**) response

(Zurich Instruments). The schematic of the measurement is shown in Fig. 5.

At first, the transfer function of the AOM is measured at a typical pump power of 9-W. A scanning modulation frequency from 10 Hz to 10 MHz is applied to the driver of AOM with a modulation amplitude of 1-V. It is noted that the relative amplitude response of pump power is nearly flat up to 100 kHz and shows a 3-dB reduction at around 1 MHz. A − 90° phase-shift of the phase response is observed at 150 kHz, as shown in Fig. 6a, b. Secondly, the transfer function of the laser cavity is resolved through measuring the amplitude and phase response of the laser output power to the pump power modulation both in the continuous wave (CW) and the mode-locking operation. The typical CW output power is 1.5 W. A peak is observed at around 45 kHz in the relative amplitude response, which is referred to the relaxation oscillation frequency (ROF) of the oscillator. It is relevant with laser cavity alignment, pump rate as well as the upper state lifetime of the gain medium. For our experiment, the theoretical ROF is estimated to be around 46 kHz, which is consistent with the measured result. When the modulation frequencies are higher than the ROF, there is a roll-off at around 40 dB per decade Hz, indicating a typical characteristic of second-order low-pass filter. The − 90° phase-shift of the phase response is also at around 43 kHz, as shown by orange in Fig. 6. Then the transfer function of the mode-locked laser is measured at typical output power of 1.5-W. The relative amplitude response exhibits a 3-dB decrease at

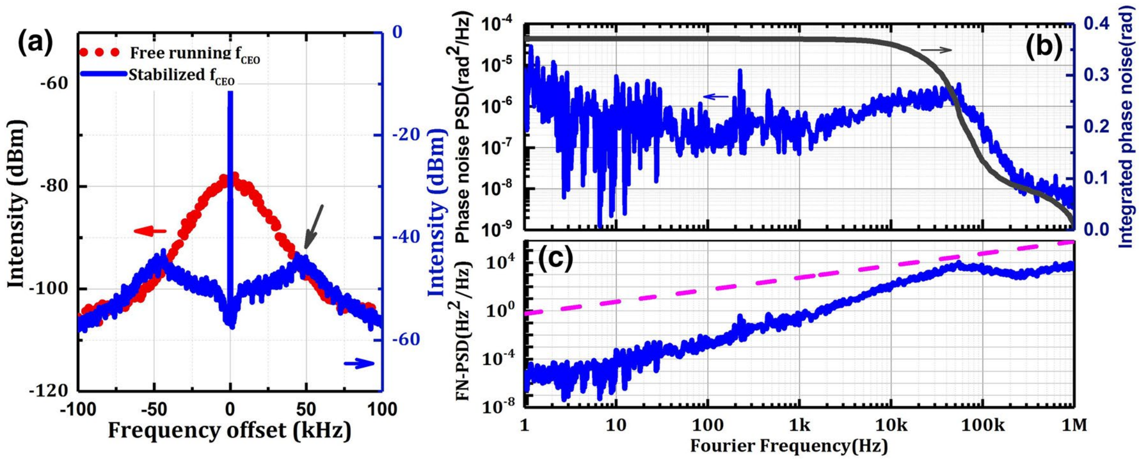

Fig. 7 **a** RF spectrum of CEO beat signal within 200 kHz span under 1 kHz RBW when phase-locked to a central frequency of 20 MHz. **b** Phase noise power spectral density of the locked f_{ceo} (left axis, bue lines) and integrated phase noise (right axis, black line). **c** Frequency noise power spectral density (FN-PSD) of the stabilized f_{ceo} and β-line (pink)

around 2 kHz and a roll-off by 18-dB per decade hertz. The − 90° phase-shift is at around 30 kHz, as shown in green line in Fig. 6. It is indicated that the AOM does not block the high frequency modulation from the pump to the laser cavity, while the ytterbium-doped laser system exhibiting low-pass filtering effect limits the servo bandwidth to the expected 45 kHz.

In order to stabilize the repetition rate of the OFC, a 2-mm long piezoelectric transducer (PZT) is mounted on the end mirror of the Yb:CYA oscillator. We measure the transfer function of PZT through demodulating the repetition rate frequency variation. As shown in Fig. 6, a scanning modulation frequency with an amplitude of 2-V is added to the PZT, and the fundamental repetition rate frequency of laser output power is detected with a photodiode, which is sent into a frequency discriminator to obtain a voltage variation for the lock-in amplifier. The relative amplitude response shows a 3-dB drop at around 200 Hz, and the − 90° phase shift also occurs at 200 Hz, indicating a servo bandwidth of hundreds of hertz.

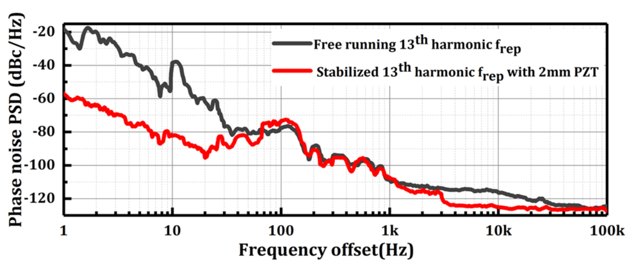

Fig. 8 Phase noise power spectral density of locked f_{rep} (red) and the free running f_{rep} (gray)

3 CEO stabilization and repetition rate stabilization

3.1 Characterization of residual phase noise of f_{ceo} and f_{rep}

For stabilizing the f_{ceo}, we phase lock the CEO beat signal to a microwave frequency synthesizer basically based on the feedback to pump power. The free running f_{ceo} detected at the end of the f-2f interferometer is first roughly tuned to around 20 MHz through a pair of wedges, and is filtered by an electronic bandpass filter and amplified to 0 dBm using an electronic power amplifier. The phase error between the noisy CEO beat signal and the external 20 MHz reference frequency is generated in a phase detector, which is sent into a proportional integral derivative (PID) electronic module. The resulting control voltage is fed back to the AOM driver to directly regulate the pump power, as depicted in Fig. 1.

As we carefully optimize the PID parameter, the f_{ceo} is tightly phase-locked to the microwave frequency standard and a distinct coherent peak with a SNR of over 45 dB under 1 kHz RBW appears at the center of 20 MHz CEO frequency, as shown in Fig. 7a. A great deal of phase noise within 50 kHz Fourier frequency of the stabilized f_{ceo} is observed to be suppressed, which is characterized in detail by the frequency resolved phase noise power spectral density (PSD) in Fig. 7b. The servo bump appears at around 45 kHz in agreement with 3-dB bandwidth laser cavity transfer function, which is determined by the upper state lifetime of Yb:CYA gain medium and cavity dynamics. The integrated phase noise of the f_{ceo} amounts to 370 mrad from 1 Hz to 1 MHz and is a bit higher than our previous results [23], which is attributed to the increased phase

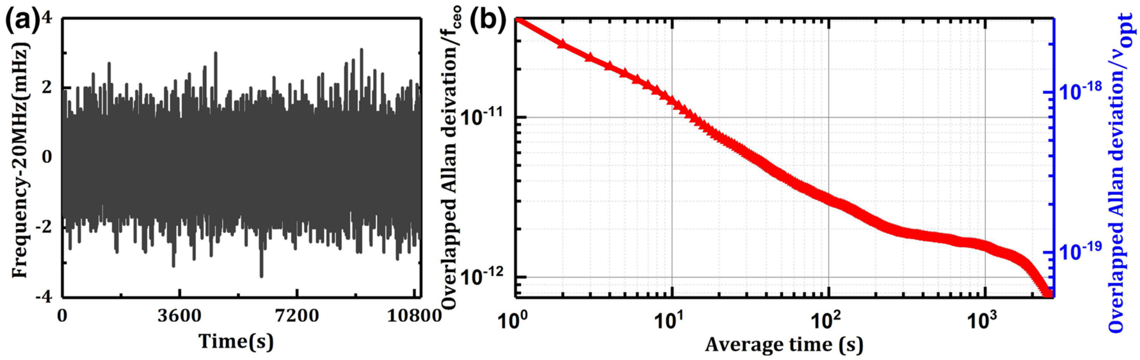

Fig. 9 **a** The frequency deviation of the stabilized f_{ceo} in 3 h recorded by the frequency counter at 1-s gate time and **b** the calculated overlapped Allan deviation corresponding to the 20 MHz central frequency and to the 1048 central optical lasing frequency (f_{opt} = 286.26 THz)

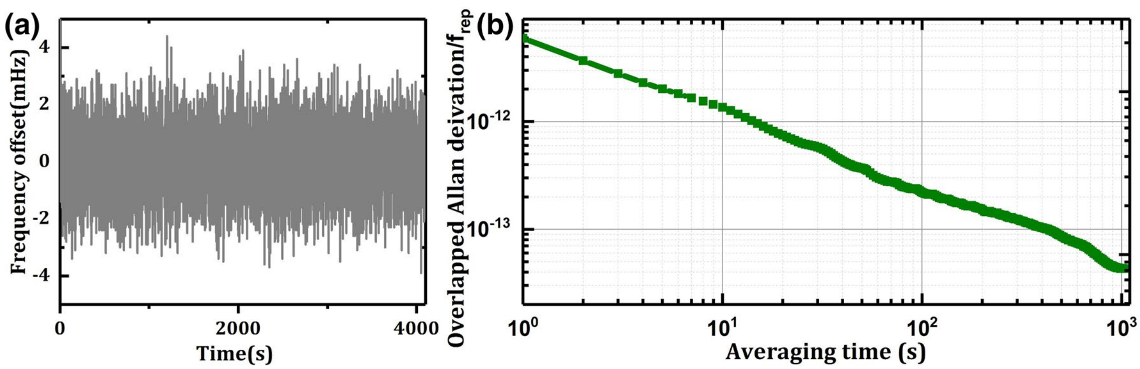

Fig. 10 **a** Frequency series of the third harmonic repetition rate. **b** The corresponding overlapped Allan deviation to repetition rate versus average time

noise coupled from the high power laser cavity as well as the limited servo bandwidth. Even so, the corresponding frequency noise power spectral density of the stabilized f_{ceo} is well below the beta-separation line, representing a tightly carrier-envelope phase locking. It also illustrates that no significant phase noise contributes to the linewidth of CEO frequency, which is ready for the comb-tooth-resolved dual comb spectroscopy [29].

For f_{rep} stabilization, the 13th harmonic repetition rate centered at 1.024 GHz was filtered and sent to a phase detector with an extra reference signal. The control voltage was amplified and added to the PZT mounted on the end mirror (Fig. 1). The phase noise PSD of the harmonic f_{rep} is characterized as shown in Fig. 8. The phase noise under 100 Hz is apparently suppressed, and the servo bump appears at 100 Hz, which is consistent with the formal measurement of transfer functions.

3.2 Characterization of long-term frequency stability of f_{ceo} and f_{rep}

We further investigate the long-term frequency stability of locked f_{ceo} utilizing a frequency counter (Agilent, 53132A) at a gate time of 1-s. Frequency fluctuations of the stabilized CEO frequency are recorded for 3-h without any adjustment. Figure 9a shows the frequency deviations to the center 20 MHz reference frequency, and the RMS is calculated to be 0.8 mHz. The fractional overlapped Allan deviation of the frequency series is analyzed corresponding the CEO frequency and the optical frequency. The overlapped fractional frequency stability of the f_{ceo} to the 1048 nm central optical wavelength is 2.9×10^{-18} at 1-s average time, indicating a tight and stable phase locking, as shown in Fig. 9b. It is the best frequency stability of 1 μm all-solid-state optical frequency combs, to the best of our knowledge. Moreover the standard deviation exhibits a typical slope of $\tau^{-1/2}$, where τ is the average time. The characteristics of the white frequency noise are presented.

The frequency deviation of the stabilized third harmonic repetition rate is observed due to the limited bandwidth of the frequency counter. The RMS of the frequency deviation is calculated to be 1.29 mHz over an hour, as shown in Fig. 10a. The fractional overlapped Allan deviation is at 10^{-12} at 1-s average time relative to the 13th harmonic repetition rate, as shown in Fig. 10b. The corresponding frequency instability of a comb line at central optical frequency is still at a relative high level, which is limited by the microwave frequency standard.

4 Conclusion

We have demonstrated a fully stabilized high power 1 µm all-solid-state bulk laser frequency comb. A high efficiency 1.5-W Yb:CYA Kerr-lens mode locked bulk laser is achieved under 980 nm fiber laser pump. An octave spanning supercontinuum peaking at 700 nm and 1400 nm is obtained with only 10% of the output power, leaving the 90% of the laser power available for other applications. A 40 dB SNR of CEO beat signal is observed at the end of a standard f-2f interferometer. The dynamic response of the laser systems as well as the PZT is fully characterized in amplitude and phase, indicating the expected modulation bandwidth and the limiting factors. CEO frequency is stabilized with a residual phase noise of 370 mrad (1 Hz–1MHZ) with a servo bandwidth of 45 kHz. The long-term frequency stability of the f_{ceo} is analyzed in terms of standard Allan deviation. The relative frequency stability corresponding to the optical frequency is 2.9×10^{-18} at 1-s average time, representing the most stable phase locking in 1 µm bulk solid state optical frequency comb. 13th harmonic of repetition rate is also tightly locked. Frequency deviation of the harmonic f_{rep} is 1.29 mHz. It is indicated that such ultra-stable watt-level optical frequency combs will serve as powerful tools for frequency comb spectroscopy and high loss time and frequency transfer.

Further works are mainly expected on the improvements of the optical coherence of the solid state laser frequency combs including stabilizing the optical frequency to an ultra-stable optical standard. Fast actuators with high bandwidth are required to suppress the high frequency noises. An electro-optical modulator (EOM) has been inserted into a solid-state Er:Yb:glass laser cavity and successfully stabilized the optical comb mode to a Hz-level cavity stabilized narrow linewidth CW laser with 700 kHz bandwidth, but at the cost of introducing amplitude modulations and significant loss into the output power [30]. With a structure of damping alloy, double PZTs scheme were able to stabilize the 1.2 GHz Yb:Y_2O_3 ceramic mode-locked laser to a Hz-level cavity stabilized CW laser with beyond 500 kHz bandwidth, holding the potential for solid state lasers based ultra-precision applications with barely no side-effect [31]. In addition, feed forward methods based on an acousto-optic frequency shifter (AOFS) outside cavity have been demonstrated to stabilize the CEO frequency of mode locked lasers and reference a CW laser to the optical frequency comb with high bandwidth and low noise, [32, 33] and are also capable of stabilize the optical comb line to a Hz-level optical standard. The latter has recently been developed to improve the mutual optical coherence of dual comb with sufficient bandwidth and longer coherent time, directly leading to applications such as precision spectroscopy, distance measurement [34, 35].

Acknowledgements The Strategic Priority Research Program of the Chinese Academy of Sciences (XDA1502040404, XDB21010400); The National Natural Science Foundation of China (NSFC) (91850209, 11434016).

References

1. J. Ma, H. Huang, K, Ning, X. Xu, G. Xie, L. Qian, K.P. Loh, D.Tang, Generation of 30 fs pulses from a diode-pumped graphene mode-locked Yb:CaYAlO4 laser. Opt. Lett. **41**, 890–893 (2016)
2. T. Udem, R. Holzwarth, T.W. Hänsch, Nature **416**, 233 (2002)
3. N. Picqué, T.W. Hänsch, Nat. Photon. **13**, 146 (2019)
4. A. Cingöz, D.C. Yost, T.K. Allison, A. Ruehl, M.E. Fermann, I. Hartl, J. Ye, Nature **482**, 68 (2012)
5. G. Porat, C.M. Heyl, S.B. Schoun, C. Benko, N. Dörre, K.L. Corwin, J. Ye, Nat. Photon. **12**, 387 (2018)
6. A. Schliesser, N. Picqué, T.W. Hänsch, Nat. Photon. **6**, 440–449 (2012)
7. G. Ycas, F.R. Giorgetta, E. Baumann, I. Coddington, D. Herman, S.A. Diddams, N.R. Newbury, Nat. Photon. **12**, 202 (2018)
8. K. Shibuya, T. Minamikawa, Y. Mizutani, H. Yamamoto, K. Minoshima, T. Yasui, T. Iwata, Opt. Express **25**, 21947 (2017)
9. F.R. Giorgetta, W.C. Swann, L.C. Sinclair, E. Baumann, I. Coddington, N.R. Newbury, Nat. Photon. **7**, 434 (2013)
10. F. Riehle, Nat. Photon. **11**, 25 (2017)
11. A. Ruehl, A. Marcinkevicius, M.E. Fermann, I. Hartl, Opt. Lett. **35**, 3015 (2010)
12. H. Fattahi, H.G. Barros, M. Gorjan, T. Nubbemeyer, B. Alsaif, C.Y. Teisset, M. Schultze, S. Prinz, M. Haefner, M. Ueffing, Optica **1**, 45 (2014)
13. N. Modsching, C. Paradis, P. Brochard, N. Jornod, K. Gürel, C. Kränkel, S. Schilt, V.J. Wittwer, T. Südmeyer, Opt. Express **26**, 28461 (2018)
14. S. Gröbmeyer, J. Brons, M. Seidel, O. Pronin, Las. Photon. Rev. **13**, 1800256 (2019)
15. H. Zhao, A. Major, Opt. Express **22**, 30425 (2014)
16. W. Tian, Y. Peng, Z. Zhang, Z. Yu, J. Zhu, X. Xu, Z. Wei, Photon. Res. **6**, 127 (2018)
17. A. Klenner, M. Golling, U. Keller, Opt. Express **22**, 11884 (2014)
18. T. Balčiūnas, O.D. Mücke, P. Mišeikis, G. Andriukaitis, A. Pugžlys, L. Giniūnas, R. Danielius, R. Holzwarth, A. Baltuška, Opt. Lett. **36**, 3242 (2011)
19. S.A. Meyer, T.M. Fortier, S. Lecomte, S.A. Diddams, Appl. Phys. B **112**, 565 (2013)
20. D. Li, X. Xu, H. Zhu, X. Chen, W.D. Tan, J. Zhang, D. Tang, J. Ma, F. Wu, C. Xia, J. Xu, J. Opt. Soc. Am. B **28**, 1650 (2011)

21. J. Ma, H.J. Ma, H. Huang, K. Ning, X. Xu, G. Xie, L. Qian, K. Ping Loh, D. Tang, Opt. Lett. **41**, 890 (2016)
22. W. Tian, C. Yu, J. Zhu, D. Zhang, Z. Wei, X. Xu, J. Xu, Opt. Express **27**, 21448 (2019)
23. Z. Zhang, H. Han, H. Wang, X. Shao, S. Fang, Z. Wei, Opt. Lett. **44**, 22 (2019)
24. S. Hakobyan, V.J. Wittwer, P. Brochard, K. Gürel, S. Schilt, A.S. Mayer, U. Keller, T. Südmeyer, Opt. Express **25**, 20437 (2017)
25. G. Genty, S. Coen, J.M. Dudley, J. Opt. Soc. Am. B **24**, 1771 (2007)
26. B. Borchers, A. Anderson, G. Steinmeyer, Las. Photon. Rev. **8**, 303 (2014)
27. N.R. Newbury, B.R. Washburn, IEEE J. Quantum Electron. **41**, 1388 (2005)
28. N. Raabe, T. Feng, M. Mero, H. Tian, Y. Song, W. Hänsel, R. Holzwarth, A. Sell, A. Zach, G. Steinmeyer, Opt. Lett. **42**, 1068 (2017)
29. G. Di Domenico, S. Schilt, P. Thomann, Appl. Opt. **49**, 4801 (2010)
30. N. Torcheboeuf, G. Buchs, S. Kundermann, E. Portuondo-Campa, J. Bennès, S. Lecomte, Opt. Express **25**, 2215 (2017)
31. T. Nakamura, S. Tani, I. Ito, M. Endo, Y. Kobayashi, Opt. Express **28**, 16118 (2020)
32. S. Koke, C. Grebing, H. Frei, A. Andderson, A. Assion, G. Steinmeyer, Nat. Photon. **4**, 462–465 (2010)
33. X.D. Shao, H.N. Han, Y.B. Su, H.B. Wang, Z.Y. Zhang, S.B. Fang, G.Q. Chang, Z.Y. Wei, AIP Adv. **9**, 11 (2019)
34. Z. Chen, M. Yan, T.W. Hansch, N. PicqueChen, Nat. Commun. **9**, 1 (2018)
35. Z. Chen, T.W. Hansch, N. Picque, Proc. Natl. Acad. Sci. USA. **116**(9), 3454–3459 (2019)